

# Cationic Gemini Surfactant as a Corrosion Inhibitor and a Biocide for High Salinity Sulfidogenic Bacteria Originating from an Oil-Field Water Tank

Ahmed Labena · Mohamed A. Hegazy ·  
Harald Horn · Elisabeth Müller

Received: 29 August 2013 / Accepted: 5 November 2013  
© AOCS 2013

**Abstract** A novel cationic gemini surfactant (NCGS) was synthesized and characterized. The inhibitory effect of NCGS was evaluated on the basis of protecting a metal surface from the salinity (5.49 % NaCl) and the activity of environmental sulfidogenic bacteria which originated from an oil-field water tank. Sulfidogenic bacterial activities were determined based on sulfide production, redox potential, changes in biofilm structures and constituents and metal corrosion rate calculations. At high surfactant concentrations, the sulfide production was completely inhibited as well as a considerable drop in the redox potential was observed in the reactor's bulk phase. A minimum inhibitory concentration of the NCGS was achieved at a concentration of 1 mM. The NCGS showed a high ability to inhibit a biofilm over the metal surface at a concentration of 0.1 mM. The lowest metal corrosion rate was detected at a concentration of 5 mM with a metal corrosion inhibition efficiency of 97 %. In addition the NCGS showed a nonspecific biocidal activity against Gram-positive and Gram-negative bacterial strains.

**Keywords** Sulfidogenic biofilm · High salinity water-tank · Cationic gemini surfactant · Microbiological corrosion · Antibacterial activity

## Introduction

Seawater is widely used in the oil and gas industries for cooling purposes, fire-fighting, oil-field water injection and desalination plants [1, 2]. Oil-field seawater is a suitable medium for sulfidogenic microorganisms as it contains a high sulfate concentration ( $\sim 20$  mM) and other nutritional requirements for microbial growth. Sulfidogenic microorganisms grow under anaerobic conditions and gain energy for growth by oxidizing organic compounds or hydrogen with sulfate being reduced to hydrogen sulfide [3]. Sulfidogenic microorganisms are a big problem in the petroleum industries where they cause iron and steel corrosion [4]. The corrosiveness of these microorganisms is due to metabolites produced such as hydrogen sulfide ( $H_2S$ ), the supposed electrochemical effect termed "cathodic depolarization", and microbial colonization (biofilm) on the metal surface. Sulfidogenic biofilms frequently show a localized attack in the form of a slimy film composed of multispecies of microbial communities, extracellular polymeric substances (EPS) and water [5]. Biofilms facilitate corrosion by trapping corrosive metabolites products such as hydrogen sulfide in close proximity to metal surfaces and then initialize localized metal corrosion [6].

There are different approaches to achieve corrosion inhibition. The applications of inhibitors are the most practical strategy for corrosion mitigation [7]. To be effective, inhibitors have to provide high microbial inhibition efficiency (biocides), displace water from the metal surface, interact with anodic or cathodic reaction sites to

---

A. Labena (✉) · E. Müller  
Chair of Urban Water Systems Engineering, Technical  
University of Munich, Am Coulombwall, 85748 Garching,  
Germany  
e-mail: labena.labena@gmail.com

M. A. Hegazy  
Egyptian Petroleum Research Institute (EPRI), Nasr City, Cairo,  
Egypt

H. Horn  
Chair of Water Chemistry and Water Technology, Karlsruhe  
Institute of Technology, Engler-Bunte-Institut,  
Engler-Bunte-Ring 1, 76121 Karlsruhe, Germany

retard oxidation and reduction corrosion reactions and to prevent the transportation of water and corrosive metabolites to the metal surface [8]. A surfactant or surface active compound is defined as a substance that, at a certain concentration, adsorbs partially or completely to the interface (metal/liquid) in a particular system [9]. A monomeric surfactant consists of a polar hydrophilic head attached to a non-polar hydrophobic tail. Dissolved surfactant molecules escape from water to an available interface due to their hydrophobic nature. A gemini surfactant represents a new class of surfactant. It is composed of at least two hydrophilic heads and two hydrophobic chain tails which are linked by spacers [9]. A gemini surfactant can protect the metal surface by adsorption to the metal/liquid interfaces. Previous studies revealed that gemini surfactants can be used as corrosion inhibitors and biocides with high metal corrosion inhibition efficiencies [10, 11].

Although corrosion inhibitors are widely used by the Egyptian Petroleum Companies, the problem of corrosion damages is still urgent and considered to be an open question. To a certain extent this is due to the fact that sulfidogenic bacteria inducing pitting corrosion are responsible for all bio-damage cases of high salinity water tanks. Therefore, a novel cationic gemini surfactant was synthesized and characterized. Investigation of the activity and effectiveness of the synthesized surfactant (corrosion inhibitor and biocide) was carried out to protect the metal surface from medium salinity and activity of environmental sulfidogenic bacteria. The sulfidogenic bacteria originated from a high salinity water tank of the Qarun Petroleum Company (QPC, Egypt). The activity of the surfactant as a biocide was discussed on the basis of sulfide production, redox potential, cultivated biofilm constituent analysis and metal corrosion rate calculations. The minimal inhibitory concentration (MIC) of the synthesized surfactant was determined from a most probable number experiment. In addition, antibacterial activity of the synthesized surfactant (against Gram-positive and Gram-negative strains) was evaluated and the MIC was calculated.

## Materials and Methods

### Synthesis of the Novel Cationic Gemini Surfactant (NCGS)

The NCGS in this study was synthesized through three steps. The first step was a quaternization reaction between 1 mol of 2-(dimethylamino)ethanol and 1 mol of 1-bromododecane in ethanol for 12 h at 70 °C [12]. The mixture was left to cool and precipitate. Then the white precipitate obtained was purified by diethyl ether and afterward recrystallized from ethanol. The second step was an

esterification reaction between 2 mol of *N*-(2-hydroxyethyl)-*N,N*-dimethyl-dodecane-1-ammonium bromide and 1 mol of phosphoric acid (in the presence of toluene as the solvent and *p*-toluene sulfonic acid as the dehydrating agent). The reaction was completed after the water had been removed from the reaction system and it was concentrated up to 2 mol. Afterward, the reaction mixture was distilled under a vacuum to completely remove the solvent. The third step, 1 mol of the resulted products was allowed to react with 1 mol of potassium hydroxide. Then reflux in ethanol for 12 h at 70 °C. The reaction mixture was left to cool for 1 h and then filtered and concentrated by ethanol evaporation. At the end the pale brown precipitate obtained was recrystallized twice from ethanol.

The chemical structure of the synthesized surfactant was confirmed by Fourier transform infrared (FTIR) and nuclear magnetic resonance (NMR) spectroscopy (Bruker, Vortex 70 and Bruker, 400 MHz NMR spectrometer, Avance DRX 400 for FTIR and NMR, respectively). The synthesized surfactant was more confirmed by <sup>31</sup>P NMR using Jeol ECA 500 NMR spectrometer at 500 MHz.

### Surface Active Properties of the Synthesized Surfactant

#### The Surface Tension ( $\gamma$ )

The surface tension was analyzed at different concentrations of the synthesized surfactant using a Du Nouy Tensiometer (Krüss Type 6). The measurement for the synthesized surfactant was done in distilled water (with a surface tension of 72 mN m<sup>-1</sup>) at 25 °C.

#### The Effectiveness ( $\pi_{CMC}$ )

The surface tension value ( $\gamma$ ) at  $C_{CMC}$  point was used to calculate the surface pressure (effectiveness) value according to the following equation [13]:

$$\pi_{CMC} = \gamma_o - \gamma_{CMC}, \quad (1)$$

where  $\gamma_o$  and  $\gamma_{CMC}$  are the surface tensions of pure water and surface tension at  $C_{CMC}$ , respectively. The most effective surfactant is one that gives the greatest lowering in the surface tension at the  $C_{CMC}$  point.

#### The Surface Excess ( $\Gamma_{max}$ )

The surface excess was calculated according to the Gibbs' adsorption equation [9]:

$$\Gamma_{max} = \left( \frac{-1}{nRT} \right) \left( \frac{d\gamma}{d \ln C} \right), \quad (2)$$

where  $\Gamma_{max}$  is the surface excess concentration of surfactant ions,  $R$  is the gas constant,  $T$  is the absolute

temperature,  $\gamma$  is the surface tension at a specific concentration,  $n$  is the number of species ions in solution and  $C$  is the concentration of surfactant. A surfactant substance that decreases the surface energy is thus present in excess or near the surface. That means the surface tension decreases with increasing activity (concentration) of a surfactant molecule.

#### The Minimum Surface Area per Molecule ( $A_{\min}$ )

The minimum surface area ( $A_{\min}$ ) is defined as an area occupied by one molecule in  $\text{nm}^2$  at the interface.  $A_{\min}$  was calculated according to the following equation [14]:

$$A_{\min} = \frac{10^{14}}{N_A \Gamma_{\max}}, \quad (3)$$

where  $N_A$  is Avogadro's number and  $\Gamma_{\max}$  ( $\text{mol m}^{-2}$ ) is the maximal surface excess of the adsorbed surfactant molecules to the interface.

#### The Conductivity ( $K$ )

The specific conductivity ( $K$ ) measurement was performed for the synthesized surfactant using a conductometer (LF 191 WTW) at 25 °C in order to evaluate the  $C_{\text{CMC}}$  value and the degree of counter ion dissociation ( $\beta$ ). The specific conductivity is linearly correlated to a surfactant concentration in both a pre-micellar and a post-micellar region [15]. The intersection point between the two lines gives the  $C_{\text{CMC}}$  value. While, the ratio between the two slopes gives the  $\beta$  value.

#### The Standard Free Energy of Micellization ( $\Delta G_{\text{mic}}^0$ )

In the charged pseudo-phase model of micellization, the standard free energy micellization ( $\Delta G_{\text{mic}}^0$ ) per mole of the synthesized surfactant was calculated according to the following equation [16]:

$$\Delta G_{\text{mic}}^0 = (2 - \beta)RT \ln C_{\text{CMC}}, \quad (4)$$

where  $\beta$  is the degree of counter ion dissociation,  $R$  is the gas constant,  $T$  is the temperature, and  $C_{\text{CMC}}$  expresses the molarity of the surfactant.

#### Application of the NCGS as a Biocide and as a Metal Corrosion Inhibitor

##### Sulfidogenic Consortia and Cultivation Conditions

A water sample with a salinity of 5.49 % was collected from the water tank of Qarun Petroleum Company (QPC), Egypt and labeled Youmna. Onsite inoculation of the water sample was done in an anaerobic selective media

**Table 1** Composition of anaerobic modified *Postgate's B* ( $P_B$ ) and *Postgate's C* ( $P_C$ ) medium

Composition ( $\text{g L}^{-1}$ )	Modified $P_B$	Modified $P_C$
$\text{KH}_2\text{PO}_4$	0.5	0.5
$\text{NH}_4\text{Cl}$	1.0	1.0
$\text{Na}_2\text{SO}_4$	1.0	4.5
$\text{CaCl}_2 \cdot 6\text{H}_2\text{O}$	–	0.06
$\text{MgSO}_4 \cdot 7\text{H}_2\text{O}$	2.0	0.06
Sodium lactate	3.5	4.42
Yeast extract	1.0	1.0
Ascorbic acid	0.1	–
Sodium thioglycolate	0.1	–
$\text{FeSO}_4 \cdot 7\text{H}_2\text{O}$	0.5	–
Sodium citrate. $2\text{H}_2\text{O}$	–	0.3
Salinity (NaCl)	54.9	54.9
pH	5.7	5.7

0.0002 % (w/v) resazurin was used as a redox potential indicator for anaerobic cultivation

(modified *Postgate's-B* medium see Table 1) according to *Postgate* [17]. Modification of *Postgate's-B* medium was done by using the original water salinity (NaCl) and pH during preparation (see Table 1). The medium was prepared, sparged with nitrogen gas and 0.0002 % (w/v) resazurin was used as a redox potential indicator for anaerobic cultivation. The medium was inoculated with 10 % (v/v) water sample and incubated at 37 °C for 14 days. Medium preparation and cultivation were achieved according to the modified *Hungate's* technique for anaerobes [18]. The appearance of a black precipitate (Ferrous sulfide) was used as a marker for sulfate reduction and as an indicator of the activity of sulfidogenic bacteria in the culture media. The inoculated sample was enriched three times under anaerobic conditions and modified *Postgate's-B* medium was used as inocula for inhibition experiments.

#### Reactors Setup and Evaluation of Sulfidogenic Activity

In order to investigate the effect of the synthesized surfactant on the sulfidogenic activity, batch reactor experiments were carried out using modified *Postgate's-C* medium (see Table 1). The *Postgate's-C* medium was modified by using the original water salinity (NaCl) and pH during preparation (see Table 1). A mild steel coupon with the chemical composition reported in Table 2 (CS1018  $3'' \times 1/2'' \times 11/6''$  strip, Cormon LTD) was used as a main iron source for the cultivated bacteria. Inhibition experiments were evaluated using different concentrations of the synthesized surfactant. In addition, two control approaches were carried out (1) blank (medium without

**Table 2** Chemical composition of mild steel coupon C1018

Chemical composition (%) (remaining: Fe)					
C	0.18	Mo	<0.01	Si	0.02
Al	0.035	Nb	<0.01	Sn	<0.01
Co	<0.01	Ni	0.01	Ti	<0.01
Cr	0.02	P	0.01	W	<0.01
Cu	0.02	Pb	<0.01	V	<0.01
Mn	0.84	S	<0.005	B	<0.0001

**Table 3** Reactors operation mode

	Reactor A	Reactor B	Reactor C
Inoculated sample	Enriched Youmna-sulfidogenic bacteria		
Temperature	37 °C		
Shaking	100 rpm		
Reactor type	Blank-reactor: reactor not inoculated with the enriched sulfidogenic bacteria Control-reactor: reactor inoculated with the enriched sulfidogenic bacteria Surfactant-reactor: reactor inoculated with the enriched sulfidogenic bacteria and exposed to different concentrations of the synthesized surfactant		
Experiment	Sulfidogenic activity	Biofilm constituents	Biofilm and metal surface analysis
Analysis	Sulfide Redox potential MPN Corrosion rate	CLSM with staining protocols to detect nucleic acids, proteins and EPS glycoconjugates in the cultivated biofilms	SEM to detect the biofilm, metal surface (after removing the biofilm), and metal surface with optimal biocide concentration
Examination day	Every 5 days: sulfide and redox potential MPN: after 5 days Corrosion rate: after 1 month (30 days)	At maximum sulfidogenic activity (high sulfide concentration in the bulk phase)	After 1 month cultivation (30 days)

bacteria) and (2) control (cultivated sulfidogenic bacteria without surfactant) (see Table 3).

Three group batch reactors (150 ml working volume) were inoculated with 3 ml enriched sulfidogenic bacteria (see Table 3). The first reactor (reactor A) was operated in order to determine the sulfidogenic activity in the bulk

phase. A separate reactor (reactor B) was implemented to evaluate the biofilm constituents using confocal laser scanning microscopy (CLSM) and staining procedure. Moreover, an additional reactor (reactor C) was operated to examine the biofilm, the metal surface (after removing the biofilm) and the metal surface inoculated with the enriched sulfidogenic bacteria and the optimum biocide concentration using scanning electron microscopy (SEM).

Samples from the bulk phase of reactor A were taken every 5 days for 1 month of cultivation to analyze the sulfidogenic activity by measuring the sulfide concentration according to the German Standard Methods [19] and redox potential using SenTix ORP electrode, WTW. The biocidal effect of the synthesized surfactants against the environmental sulfidogenic-bacteria was evaluated by determine the minimum inhibitory concentration (MIC). The MIC is defined as the lowest concentration of antimicrobial agent that inhibits the development of visible microorganism growth [20]. Samples were taken from the bulk phase of reactor A after 5 days cultivation and tested for viable bacterial counts using the most probable number (MPN) method [21]. At the end of 1 month of incubation (30 days), the coupons were taken from reactor A and immersed in Clarke solution (1 L 36 % HCl, 20 g Sb<sub>2</sub>O<sub>3</sub> and 50 g SnCl<sub>2</sub>) for 10–15 s, washed with deionized water, ethanol and finally dried in a desiccator. Afterward, the dried coupons were weighed and the weight loss was determined by comparison of the weights of the coupons after and before the inhibition experiments. The corrosion rate (gm<sup>-2</sup> day<sup>-1</sup>) [22] and metal corrosion inhibition efficiency [23] were calculated from the weight loss results.

CLSM with staining protocol was used to detect the change in bacterial cells and EPS distribution within the sulfidogenic-biofilm matrix in the presence and absence of the synthesized surfactant. At maximum sulfidogenic-activity (the highest sulfide value in the bulk phase), the mild steel coupons with the attached biofilms were taken from reactor B and immersed first in 0.85 % NaCl to remove the planktonic cells. For the detection/quantification of bacteria, the nucleic acid stain SYTO9 (Invitrogen, Eugene, USA) was used according to the protocol described by Neu [24]. *Aleuria aurantia* lectin (AAL, LINARIS Biologische Produkte GmbH, Wertheim-Bettingen, Germany) labeled with AlexaFluor 633 (Invitrogen/Molecular Probes, Eugene, USA) was applied to stain glycoconjugates. Proteins were stained with SYPRO Orange (Invitrogen/Molecular Probes, Eugene, USA) according to the protocol described by Lawrence et al. [25]. A Zeiss LSM510 META (Carl Zeiss Micro-Imaging GmbH, Jena, Germany) was used to create image stacks, adjusted by the AIM software (v. 3.2, Carl Zeiss Micro Imaging GmbH, Jena, Germany). For excitation, two wavelengths were used: 488 and 633 nm that are related to the stains used.

A  $63 \times 0.95$  numerical aperture (NA) water immersion lens was applied for *in-situ* observation of biofilms over the coupons. For each sample, five microscopic fields were selected randomly and scanned for nucleic acids, EPS glycoconjugates and proteins. The pinhole was adjusted for all channels with an identical value to the stack slice thicknesses of  $0.79 \mu\text{m}$  [26]. For image analysis, the software ImageJ (v.1.39i, <http://rsb.info.nih.gov/ij/index.html>) was used, image analysis and calculation details were documented by Wagner et al. [27]. The coverage ( $C$ ) of each single image of the image stack was quantified by the ImageJ software. The average coverage ( $\bar{C}_{\text{stack}}$ ) was calculated for each image stack from the first slice ( $n = 1$ ) where the average coverage equal to 0.1 % of the last slice ( $n = n_{\text{max}}$ ) where the average coverage was equal to 0.1 % according to the following equation [27],

$$\bar{C}_{\text{stack}} = \frac{1}{n_{\text{max}}} \sum_{n=1}^{n=n_{\text{max}}} C \quad (5)$$

Then the mean average coverage values of the five scanned microscopic fields on the same coupon was calculated and used to evaluate the change in the nucleic acids, EPS glycoconjugates and proteins in different biofilms.

The biofilms, metal surfaces (after removing the biofilm) and the metal surfaces inoculated with the enriched sulfidogenic bacteria and the optimum biocide concentration were examined using scanning electron microscopy (SEM) model Leica/Cambridge Stereo scan 360 at magnifications ranging from  $50\times$  to  $10,000\times$  and operated at an acceleration voltage of 20 V. After 1 month incubation time, the metal surface samples were removed from reactor C, fixed with 3 % glutaraldehyde PBS, pH 7.3–7.4 for 4 h, washed two times with PBS (5 min each), rinsed with distilled water for another two times (5 min each) and then dehydrated using an ethanol gradient (50, 75, 95 and 99 %) for 10 min before being finally stored in the desiccator.

#### Antibacterial Activity of the Synthesized Surfactant

The antibacterial (biocidal) activity of the synthesized surfactant was tested against different bacterial strains (DSMZ: Deutsche Sammlung von Mikroorganismen und Zellkulturen) as follows: Gram-positive bacteria (*Staphylococcus aureus* DSM 3463) and Gram-negative bacteria (*Pseudomonas aeruginosa* DSM 50071, *Escherichia coli* DSM 30083). The antibacterial activity of the synthesized surfactant was determined by a modified agar-well diffusion method [28]. In this method, nutrient agar plates were seeded with the tested microorganism by streaking over the agar plates. A sterile 10-mm borer was used to cut three wells of equidistance in each of the plates; 0.2 ml of

synthesized surfactant was introduced into the wells. The plates were incubated at  $37^\circ\text{C}$  overnight. The antibacterial activity was evaluated by measuring the diameter of zones of inhibition (in mm). In addition, a standard tetracycline solution was used as a positive control and sterile water was used as a negative control.

## Results and Discussion

### Confirmation of Chemical Structure of the Synthesized NCGS

The chemical structure of the NCGS was confirmed by FTIR and NMR (proton and carbon, and phosphorous) spectroscopy.

#### FTIR Spectra

FTIR spectra of the synthesized NCGS demonstrated that the characteristic bands for the alkyl moiety are  $2,922.65$ ,  $2,853.03 \text{ cm}^{-1}$  for asymmetric and symmetric stretching (CH), respectively. While at  $1,377.90 \text{ cm}^{-1}$  for symmetric bending ( $\text{CH}_3$ ), at  $1,466.93 \text{ cm}^{-1}$  for symmetric bending ( $\text{CH}_2$ ) and at  $720.52 \text{ cm}^{-1}$  for  $-(\text{CH}_2)_n-$  rock.  $\text{R}_4\text{N}^+$  appeared as a band at  $1,058.00 \text{ cm}^{-1}$ . In addition, there was a band at  $1,097.76 \text{ cm}^{-1}$  for P–O–C aliphatic and a band at  $907.64 \text{ cm}^{-1}$  corresponding to ionic phosphate and one at  $1,150.64 \text{ cm}^{-1}$  for P=O stretching. The FTIR spectrum confirmed the expected functional groups in the synthesized NCGS.

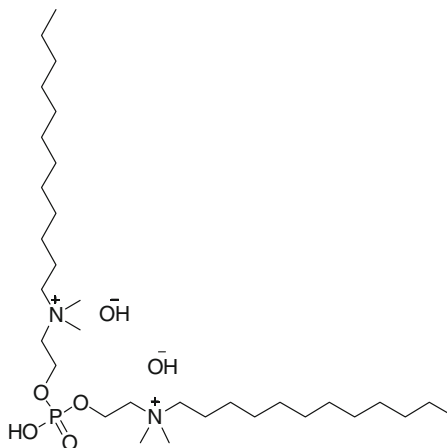
#### NMR Spectra

The  $^1\text{H}$ -NMR (DMSO) spectrum of the synthesized NCGS showed different bands at  $\delta = 0.88 \text{ ppm}$  (t, 3H,  $\text{NCH}_2\text{CH}_2(\text{CH}_2)_9\text{CH}_3$ );  $\delta = 1.23 \text{ ppm}$  (m, 18H,  $\text{NCH}_2\text{CH}_2-(\text{CH}_2)_9\text{CH}_3$ );  $\delta = 1.73 \text{ ppm}$  (m, 2H,  $\text{NCH}_2\text{CH}_2(\text{CH}_2)_9\text{CH}_3$ );  $\delta = 3.35 \text{ ppm}$  (t, 2H,  $\text{NCH}_2\text{CH}_2-(\text{CH}_2)_9\text{CH}_3$ ); at  $3.45 \text{ ppm}$  (s, 3H,  $\text{NCH}_3$ );  $\delta = 3.70 \text{ ppm}$  (t, 3H,  $\text{NCH}_2\text{CH}_2\text{OP}$ );  $\delta = 4.11 \text{ ppm}$  (t, 2H,  $\text{NCH}_2\text{CH}_2\text{OP}$ ).

The data of the  $^1\text{H}$ -NMR spectrum confirmed the expected hydrogen proton distribution in the synthesized NCGS.

The  $^{13}\text{C}$ -NMR ( $\text{CDCl}_3$ ) spectrum of the synthesized NCGS presented different bands at  $\delta = 14.07 \text{ ppm}$  ( $\text{NC H}_2\text{CH}_2\text{CH}_2(\text{CH}_2)_6\text{CH}_2\text{CH}_2\text{CH}_3$ );  $\delta = 18.02 \text{ ppm}$  ( $\text{NCH}_2\text{CH}_2\text{CH}_2-(\text{CH}_2)_6\text{CH}_2\text{CH}_2\text{CH}_3$ );  $\delta = 23.19 \text{ ppm}$  ( $\text{NCH}_2\text{CH}_2\text{CH}_2(\text{CH}_2)_6\text{CH}_2\text{CH}_2\text{CH}_3$ );  $\delta = 29.27 \text{ ppm}$  ( $\text{NCH}_2\text{CH}_2\text{CH}_2-(\text{CH}_2)_6\text{CH}_2\text{CH}_2\text{CH}_3$ );  $\delta = 26.55 \text{ ppm}$  ( $\text{NCH}_2\text{CH}_2\text{CH}_2(\text{CH}_2)_6\text{CH}_2\text{CH}_2\text{CH}_3$ );  $\delta = 23.18 \text{ ppm}$  ( $\text{NCH}_2-\text{CH}_2\text{CH}_2-(\text{CH}_2)_6\text{CH}_2\text{CH}_2\text{CH}_3$ );  $\delta = 66.21 \text{ ppm}$  ( $\text{NCH}_2\text{CH}_2\text{CH}_2-(\text{CH}_2)_6\text{CH}_2\text{CH}_2\text{CH}_3$ ); at  $\delta = 51.93 \text{ ppm}$  ( $\text{NCH}_3$ );

**Fig. 1** Chemical nomenclature and structure of the synthesized surfactant according to IUPAC



*N,N'*-(((hydroxyphosphoryl)bis(oxy))bis(ethane-2,1-diy))bis(*N,N*-dimethyldodecan-1-ammonium) hydroxide

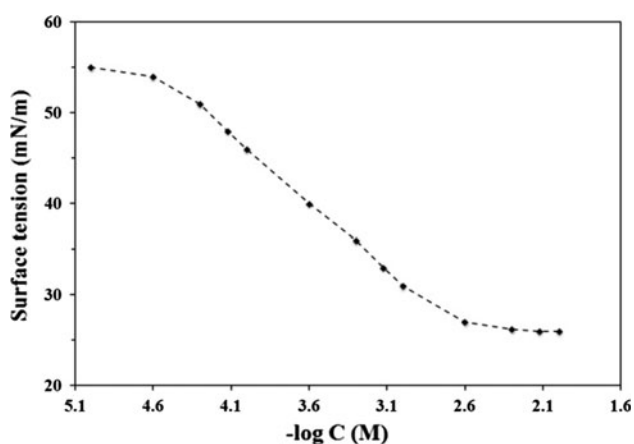


**Fig. 2** The surface tension of the synthesized surfactant at different concentrations in water at 25 °C

$\delta = 58.25$  ppm ( $\underline{\text{NCH}_2\text{CH}_2\text{O}}$ );  $\delta = 55.95$  ppm ( $\underline{\text{NCH}_2\text{CH}_2\text{O}}$ ).

The data of  $^{13}\text{C}$ -NMR spectra confirmed the expected carbon distribution in the synthesized NCGS.

The  $^{31}\text{P}$ -NMR (DMSO) spectrum of the synthesized NCGS showed characteristic signal at  $\delta_p -0.5114$  ppm.

The nomenclature and the chemical structure of the synthesized NCGS are given according to international union of pure and applied chemistry (IUPAC) (see Fig. 1).

#### Surface Active Properties of the Synthesized NCGS

##### The Surface Tension ( $\gamma$ )

The changes in the surface tension ( $\gamma$ ) values of the synthesized surfactant at different concentrations are presented in Fig. 2. Significant decreases in the surface tension were observed with increasing surfactant concentrations. Afterward the curves break rapidly at relatively low surfactant concentrations and continue to decrease slowly as the

concentration increases. The  $C_{\text{CMC}}$  value ( $2.3 \times 10^{-3}$  mol dm $^{-3}$ ) was determined from the break points in the  $\gamma$ -log  $C$  plots of the synthesized surfactant [14]. This behavior shown by the surfactant molecule in the solution is common and is used to determine its purity and  $C_{\text{CMC}}$  value (see Table 4).

##### The Effectiveness ( $\Pi_{\text{CMC}}$ )

The effectiveness of the synthesized NCGS is good for lowering the surface tension of water to the present value (Table 4). The synthesized NCGS showed higher effectiveness ( $45$  mN m $^{-1}$ ) in comparison to other cationic gemini surfactants ( $28.2$ – $33.7$  mN m $^{-1}$ ) at the  $C_{\text{CMC}}$  points [29].

##### The Surface Excess ( $\Gamma_{\text{max}}$ )

The surface excess ( $\Gamma_{\text{max}}$ ) data show that by increasing the hydrophobic chain length, as in the case of the synthesized NCGS (see Table 4), the hydrophobicity increases. Thus, the synthesized surfactant molecules are directed to the interface and therefore, the surface energy of the solution decreases. This leads to an increase in the maximum surface excess.

##### The Minimum Surface Area per Molecule ( $A_{\text{min}}$ )

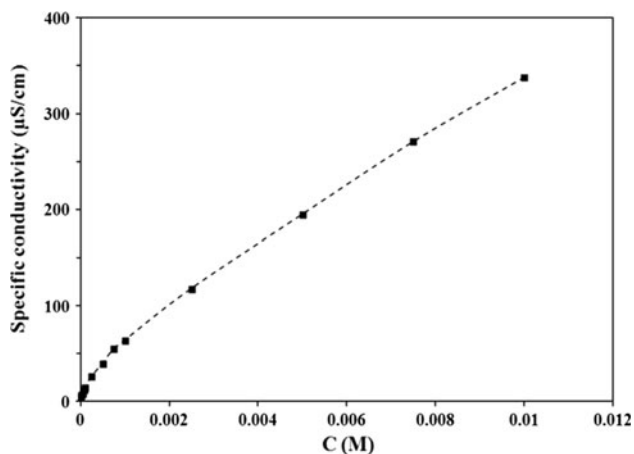
Results reported in Table 4 reveal that the surface pressure ( $\pi_{\text{CMC}}$ ) of the synthesized NCGS increases with decreasing the minimum surface area ( $A_{\text{min}}$ ) of the adsorbed surfactant molecules as previously reported [29].

##### Conductivity Measurements ( $K$ )

The  $C_{\text{CMC}}$  value calculated from the specific conductivity figure (Fig. 3) was in agreement with that obtained using

**Table 4** Critical micelle concentration ( $C_{CMC}$ ), surface tension at  $C_{CMC}$  ( $\gamma_{CMC}$ ), effectiveness ( $\pi_{CMC}$ ), maximum surface excess ( $\Gamma_{max}$ ), and minimum area ( $A_{min}$ ), the degree of counter ion dissociation ( $\beta$ ) and free energy of micellization ( $\Delta G_{mic}^0$ ) of the synthesized surfactant at 25 °C

Inhibitor	$C_{CMC}$ (mol dm <sup>-3</sup> )	$\gamma_{CMC}$ (mN m <sup>-1</sup> )	$\pi_{CMC}$ (mN m <sup>-1</sup> )	$\Gamma_{max} \times 10^{10}$ (mol m <sup>-2</sup> )	$A_{min}$ (nm <sup>2</sup> )	$\beta$	$\Delta G_{mic}^0$ (kJ mol <sup>-1</sup> )
NCGS	$2.3 \times 10^{-3}$	27	45	6.31	0.26	0.26	-23.18

**Fig. 3** The electrical conductivity of the synthesized surfactant at different concentrations in water at 25 °C

the surface tension result (see Fig. 2). Increasing in the conductivity of the synthesized NCGS was related to increases in the cation bulkiness [8].

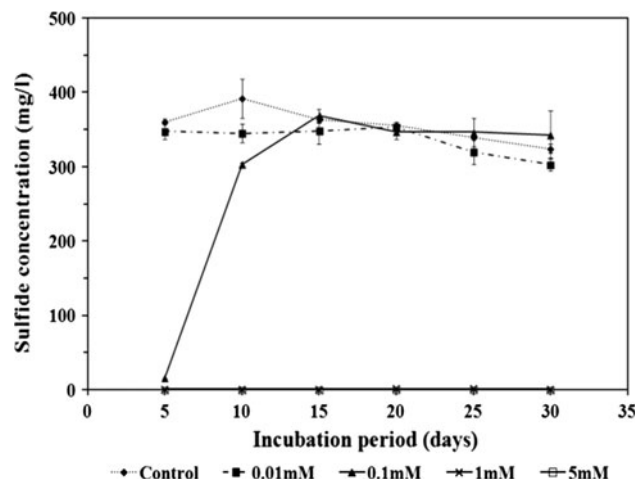
#### The Standard Free Energy of Micellization ( $\Delta G_{mic}^0$ )

Results listed in Table 4 show that the negative value of  $\Delta G_{mic}^0$  of the synthesized NCGS indicated that there is a tendency of the synthesized surfactant molecules to be adsorbed at the interface [30].

#### Inhibition of environmental sulfidogenic bacterial activity using the novel cationic gemini surfactant (NCGS)

The water sample was enriched and used as an inoculum for biofilm cultivation. The dissimilatory sulfite reductase- $\beta$  subunit (*dsr $\beta$* ) based on the denaturing gradient gel electrophoresis (DGGE) was used to identify the sulfidogenic community's composition directly from the original water sample (W) and from its cultivated biofilm (CB). The DGGE pattern of the Youmna sample (data not shown) shows a reduction in microbial diversity from nine bands in W to one band in CB. The change in the DGGE pattern in W and CB might be attributed to the selective cultivation conditions which did not reflect the *in-situ* water properties such as organic, inorganic contents and cultivation temperature [31, 32].

The most detected sulfidogenic bacteria were *Desulfovibrio* genus (phylum Proteobacteria, class

**Fig. 4** Sulfidogenic bacterial activities shown on the basis of the sulfide production in the bulk phase for the different reactors. The results shown are mean values of duplicates with corresponding standard deviations

Deltaproteobacteria). No Archaea with a *dsr $\beta$* -gene were detected in the DGGE band sequences.

According to the  $C_{CMC}$  value of the synthesized NCGS (see Table 4), the surfactant concentration-ranges were selected. The  $C_{CMC}$  value of the NCGS was  $2.3 \times 10^{-3}$  mol dm<sup>-3</sup> therefore the concentration-ranges were chosen as 0.01, 0.1, 1 and 5 mM. The enriched inoculum of the cultivated reactors had initial MPN count of  $2.9 \times 10^8$  ml<sup>-1</sup>.

Results presented in Fig. 4 showed that there was a strong sulfide production in the control reactor and the sulfidogenic-reactor treated with surfactant at a concentration of 0.01 mM. Sulfide production was gradually decreased by applying different concentrations of the surfactant (biocide) throughout the experiment. The sulfide result indicates the growth of the sulfidogenic bacteria which growing by either oxidizing organic compounds or utilizing hydrogen as an electron donor with sulfate being reduced to hydrogen sulfide [33]. At a concentration of 0.1 mM NCGS, the Youmna-sulfidogenic activity was inhibited at the beginning, but after 5 days it started to resist the biocide effect. Reactor inoculated with the Youmna-sulfidogenic bacteria showed no sulfide production at high surfactant concentrations of 1, 5 mM. No sulfide production means that there is no sulfidogenic activity in the bulk phase or over the metal surface. The inhibition of sulfide production is an important factor to protect the

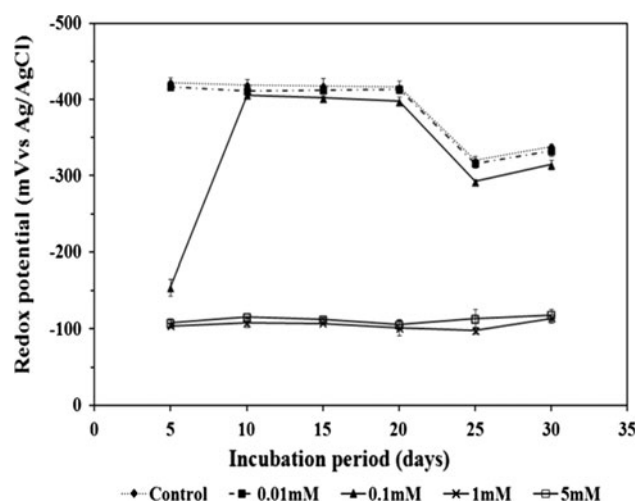


**Fig. 5** Sulfidogenic bacterial activities shown on the basis the redox potential for the different reactors. The results shown are mean values of duplicates with corresponding standard deviations

metal surface from microbial metal corrosion. Hydrogen sulfide can accelerate corrosion of metals by being source of bound protons and by precipitation of  $\text{Fe}^{2+}$  as  $\text{FeS}$  [34]. It has also been proposed that the iron sulfide film that precipitates over the metal surface plays an important role in the initiation of pitting corrosion of metal. In this respect, applying the synthesized surfactant at high concentrations of 1, 5 mM protects the metal surface from the sulfidogenic bacterial activity.

The measured redox potential in the different reactors (Fig. 5) is in agreement with the sulfidogenic activity determined by sulfide production. Most sulfidogenic bacteria are strictly anaerobic and start to reduce sulfate at a redox potential below  $-100$  mV [17]. For the control reactor and the reactors treated with NCGS at concentrations of 0.01 and 0.1 mM the redox potential measured was optimal for the sulfidogenic bacterial growth. While at high NCGS concentrations 1, 5 mM the measured redox potential of the Youmna-sulfidogenic bacteria was increased up to  $-100$  mV. The sulfide and redox potential results demonstrate that at high surfactant concentrations, the sulfate reduction reaction was completely inhibited causing no sulfide production and a considerable drop in the redox potential in the reactor's bulk phase.

Results presented in Table 5 showed the minimum inhibitory concentration (MIC) of the synthesized surfactant is detected at a concentration of 1 mM. With increasing the synthesized surfactant concentrations no sulfidogenic bacterial growth was detected. At a lower concentration of 0.01 mM NCGS, there is no significant biocidal effect against Youmna-sulfidogenic bacteria. However at a concentration of 0.1 mM NCGS, the Youmna-sulfidogenic bacterial growth was partially inhibited.

**Table 5** Evaluation of the most probable number (MPN) of the cultivated reactors

Cultivated reactors	MPN ( $\text{cell ml}^{-1}$ )
Control	$2.6 \times 10^9$
0.01 mM	$2.4 \times 10^9$
0.10 mM	$1.1 \times 10^5$
1.00 mM	No growth
5.00 mM	No growth

In general, the biocidal activity of the synthesized surfactant depends on the alkyl chain length that is increased in the synthesized NCGS in comparison to the monomeric surfactant. The biocidal effect took place at concentrations of surfactant below the  $C_{CMC}$  and is due to the individual molecules and not to the aggregates [17].

The hypothesized biocidal effect of the synthesized surfactant against bacterial cells can be explained as an electrostatic interaction and physical disruption. Electrostatic interaction between the negatively charged cell membrane (lipoprotein) and the positively charged NCGS two ammonium groups ( $\text{R}_4\text{N}^+$ ). A physical disruption occurs when hydrophobic chains (alkyl groups) penetrate into the bacterial cell membrane. That happens because of similarity of the cell membrane constituents and the hydrophobic chains of the synthesized surfactants. Penetration of the cell membrane leads to damage of the selective permeability of the cell, disturbs the metabolic pathway within the cytoplasm and then death of the microorganism as has been reported previously [11, 35]. The NCGS contains two hydrophilic groups and two hydrophobic groups linked by spacer. This spacer contains one phosphorous and three oxygen atoms. It has been reported that phosphorus containing compounds are commonly used to inhibit metal corrosion in aqueous environments [36]. Their use is considered to be risk free due to their low toxicity [37].

The sulfidogenic activities shown were detected in the bulk phase, not over the metal surface. Therefore, in order to characterize the possible changes in the biofilm structure and constituents over the metal surface after surfactant application, CLSM and staining procedures were used. Biofilm development was only detected in the control reactor and reactor inoculated with the synthesized NCGS at a concentration of 0.01 mM (Fig. 6). At a concentration of 0.01 mM NCGS, the Youmna-biofilm microbial population (nucleic acids) does not reveal significant changes in comparison to the control biofilm. When EPS components were changed, EPS glycoconjugates were reduced and the proteins increased. The explanation of EPS components changing by applying the biocide is a defensive behavior of the microbial population. It has been reported

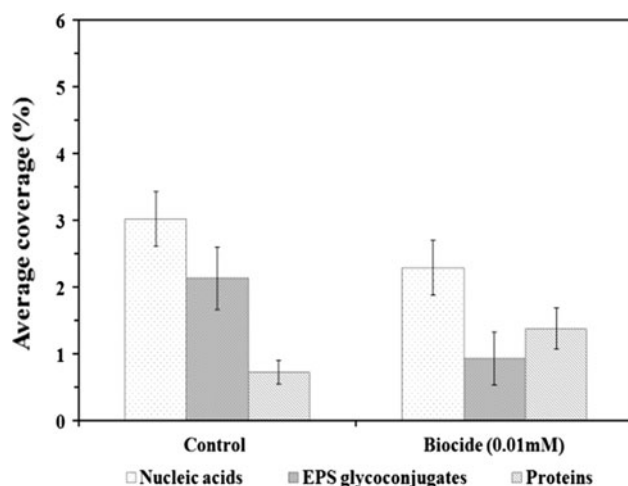


**Fig. 6** The changing of nucleic acids, EPS glycoconjugates and proteins of the sulfidogenic biofilms control reactor and the biocide reactor. The figure shows the average coverage of five randomly selected areas of the cultivated biofilms with corresponding standard deviations

that, the natural response of microorganisms upon exposure to a toxic environment is to stimulate the production of EPS. This natural response has been detected when the SRB biofilm is exposed to seawater containing toxic heavy metals and it started to produce more protein than polysaccharides [38]. However the biofilm development on the metal surface at a concentration of 0.1 mM NCGS was completely inhibited, no complete inhibition was detected in the bulk phase.

Increasing the NCGS concentrations (0.1, 1, 5 mM) completely inhibited Youmna-sulfidogenic biofilms development over the metal surface. The explanation of this result, at high concentrations of 1, 5 mM the synthesized surfactant, the metal surface was completely protected not only from the planktonic bacterial cells, as confirmed by the fact that there was no sulfide production and drop in the redox potential in the bulk phase, but also from the biofilms development.

At the end of the 1 month cultivation (30 days), the metal corrosion rate of the coupons was calculated (Fig. 7). The higher metal corrosion rate of the Youmna blank-reactor (without biomass) in comparison to the Youmna control-reactor (inoculated with Youmna-sulfidogenic consortia), show that the medium salinity (5.49 % NaCl) caused metal corrosion in the blank-reactor and the sulfidogenic biofilm in the control-reactor protected the metal surface from the harmful chloride anion effect as postulated before [34, 39, 40]. It has been reported that metal corrosion in an aqueous medium containing NaCl (artificial seawater) proceeds by chemisorption of chloride ions on the metal surface. There are two theories of chloride anion/metal surface interaction. The first theory is the oxide-film,

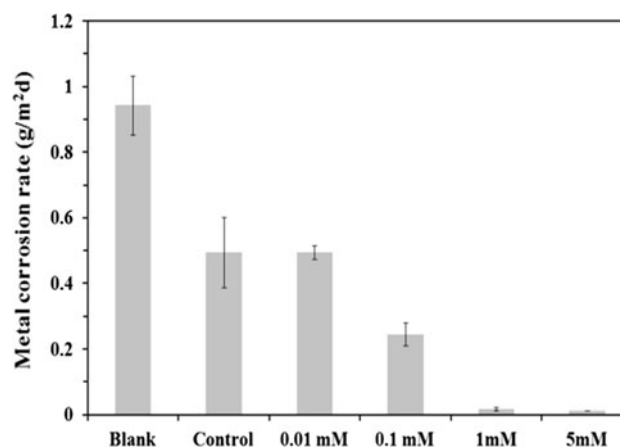
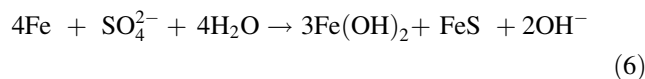


**Fig. 7** The corrosion rate of sulfidogenic bacteria is demonstrated. The blank reactor (media without bacteria), the control reactor (inoculated with the sulfidogenic bacteria without the inhibitor) and the reactors with different inhibitor concentrations. The results shown are the mean values of duplicates with corresponding standard deviations

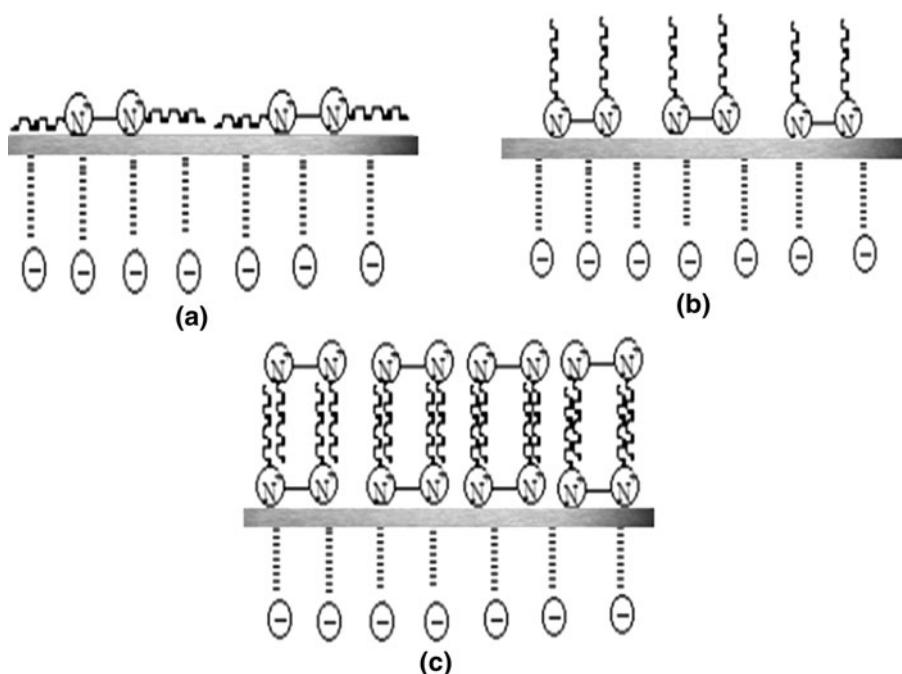
where the chloride anion penetrates the oxide film of the metal surface through pores or defects easier than do other ions. In addition it may colloiddally disperse the oxide film and increase its permeability. On the other hand, according to the adsorption theory, once the chloride anion is in contact with the metal surface, it favors hydration of the metal ions and increases the ease with which metal ions enter into solution. Then the adsorbed chloride ions lead to pit and crevice corrosion [41]. The role of chloride in the metal corrosion process is unique. It can be reacted again and again and hence even a small number of chloride anions can sustain the metal corrosion process. Thus the iron-chloride reaction is self-perpetuating and the free chloride serves as a reaction catalyst [42].

The mechanisms of metal corrosion in the presence of sulfidogenic bacteria in the bulk phase and over the metal surface (control reactors) are complex. In an anaerobic environment, sulfidogenic bacteria utilize hydrogen (as an electron donor) with sulfate (as an electron acceptor) being reduced to sulfide. In this respect, Von Wolzogen Kuhr and Van der Vlugt [43] suggested the following corrosion reaction:



This reaction is described as a cathodic depolarization theory. Based on this theory, sulfidogenic bacteria increase the metal corrosion rate by continuous consume the atomic hydrogen that accumulated at the cathode by a hydrogenase enzyme. Therefore it leads to increasing the metal dissolution. Some researchers [44, 45] suggested that the metal corrosion rate increases as a result of the cathodic reduction of  $\text{H}_2\text{S}$ :

**Fig. 8** Diagram of the adsorption mechanism of a cationic gemini surfactant on the metal surface. Adapted from Ref. [49]



and the anodic reaction is stimulated by the formation of iron sulfide which plays an important role in initiating the pitting corrosion of metal:



Directly on the metal surface, the metal corrosion rate was related to the sulfidogenic bacteria attached to the surface. It has been hypothesized that EPS have the ability to entrap metal ions by binding carboxylic groups of the exopolysaccharides and phosphate groups of the nucleic acids. This binding influences the electrochemical behavior of a metal through formation of metal corrosion cells and galvanic coupling [46, 47]. In addition, the sulfidogenic biofilm increases corrosion by trapping corrosive sulfide in close proximity to the metal surfaces [6].

The application of surfactant at different concentrations gradually decreased the metal corrosion rate. The lowest metal corrosion rate of the Youmna reactors was achieved at a concentration of 5 mM with a metal corrosion inhibition efficiency of 97 %. At this concentration, the synthesized surfactant shows a biocidal effect against the environmental sulfidogenic bacteria in the bulk phase and over the metal surface. In a medium with high salinity (5.49 % NaCl) with free Youmna-sulfidogenic bacterial activity, the metal surface corrodes by the effect of corrosive chloride anions. In this respect the application of the synthesized surfactant protects the metal surface from the chloride corrosion effect. Therefore the hypothesized metal surface corrosion inhibition behavior of the synthesized surfactant against the cultivated medium salinity

can be explained as adsorption of the surfactant molecules and formation of a tight surfactant layer at the metal/liquid interface and not due to the micelles [10]. The surfactant layers which are adsorbed to the metal surface act as an inhibitive shield and protect the metal surface from the surrounding environment [48]. Two types of adsorption may take place (physical and chemical). The procedure of physical adsorption requires the presence of an electrically charged metal surface and charged species in the bulk phase. The chemisorption process involves a charge transfer or charge sharing between the inhibitor molecules and the metal surface. The presence of an inhibitor molecule that has relatively loosely bound electrons or heteroatoms with lone-pair electrons together with a transition metal have a vacant and low-energy electron orbital, promotes this adsorption. The NCGS contains two hydrophilic groups and two hydrophobic groups linked by a spacer. This structure reflects three different types of adsorption: (1) at low gemini surfactant concentrations, the adsorption takes place by a horizontal binding of the gemini surfactant to the metal surface (Fig. 8a). This adsorption attitude is favored by an electrostatic interaction between the two ammonium groups ( $\text{R}_4\text{N}^+$ ) and the cathodic sites on the one hand and the hydroxide ion on the anodic sites on the other hand. (2) At high gemini surfactant concentration, a perpendicular adsorption occurs as a result of an inter-hydrophobic chain interaction (Fig. 8b). (3) With further increase of gemini surfactant concentration, up to the  $C_{\text{CMC}}$  value, an efficiency plateau appears (Fig. 8c) [49].

The corrosion inhibition efficiency was confirmed by applying SEM to the metal surface. Figure 9a shows an SEM image of a carbon steel surface after 1 month incubation with the Youmna-sulfidogenic bacteria which was

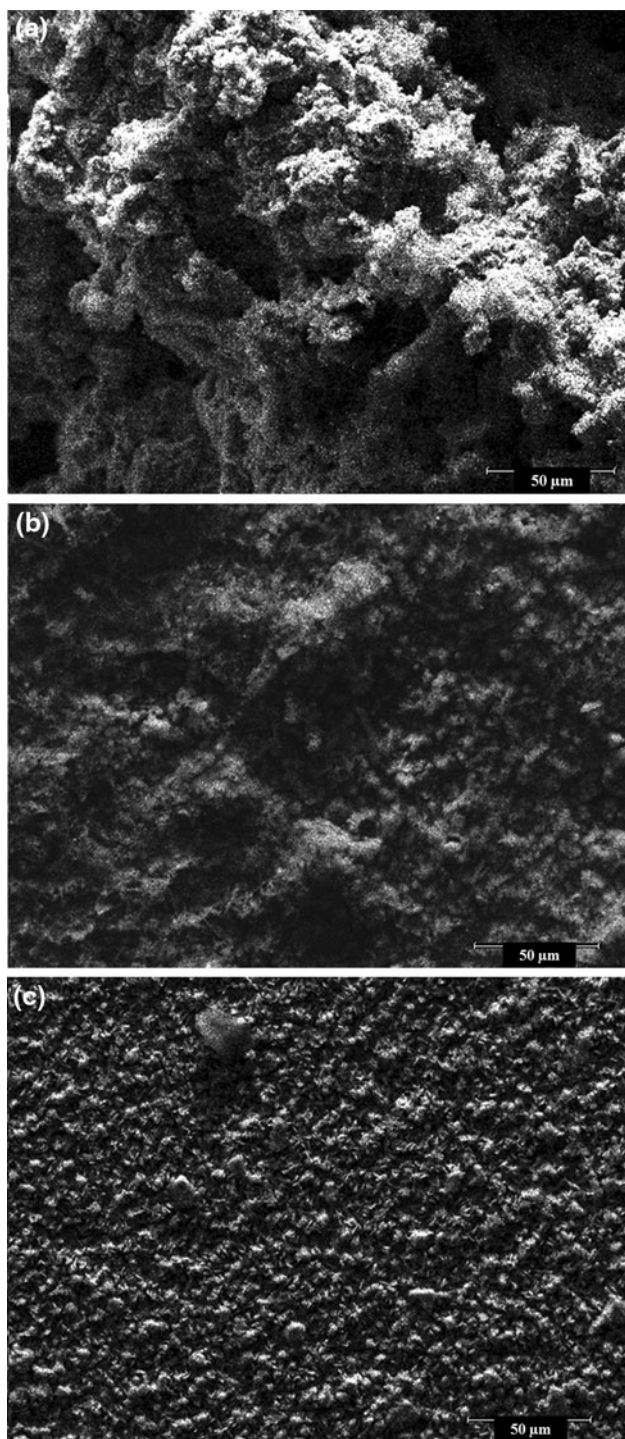


**Fig. 9** SEM images of, **a** the sulfidogenic biofilm over the mild steel coupon, **b** the metal surface after removing the biofilm and **c** 5 mM NCGS with the enriched Youmna-sulfidogenic bacteria. Scale bar 50 µm

cultivated at a medium salinity of 5.49 % NaCl. The biofilm images showed that the metal surface was completely covered with biofilm. After removing the biofilm, the surface was damaged as the effect of the cultivated biofilm

**Table 6** Antibacterial activity of the synthesized surfactant

Biocide	Concentration (mM)	<i>S. aureus</i> (DSM 3463) (mm)	<i>P. aeruginosa</i> (DSM 50071) (mm)	<i>E. coli</i> (DSM 30083) (mm)
NCGS	0.01	0	0	0
	0.10	15.8 ± 0.2	0	0
	1.00	28 ± 0	23 ± 0	15.3 ± 0.5
	5.00	39 ± 0	24.8 ± 0.2	28 ± 0
	10.00	40 ± 0	29.1 ± 0.2	31 ± 0

0 mm no effect as a resistance of the cultivated bacteria to the antimicrobial agent

at high salinity that induces metal corrosion (Fig. 9b). However Fig. 9c showed the surface of another steel sample after cultivation for the same period in a medium containing 5 mM NCGS and inoculated with the enriched Youmna-sulfidogenic bacteria. The SEM image revealed that the surfaces are free from pits and completely covered with the inhibitors. This result indicates a good protective inhibitor film over the steel surface and confirms the highest inhibition efficiency of the synthesized NCGS.

Results reported in Table 6 indicate that, the synthesized surfactant has a nonspecific antibacterial activity. The synthesized NCGS showed antibacterial (biocidal) activity not only against environmental sulfidogenic bacteria but also against Gram-positive (*S. aureus*) and Gram-negative (*E. coli* and *P. aeruginosa*) species. The antimicrobial activity depends on the ammonium groups ( $R_4N^+$ ) and hydrophobic alkyl groups of the synthesized surfactant. It has been reported that increasing the hydrophobicity as in the gemini surfactant leads to an increase in the biocidal activity [50]. The hypothesized explanation of the non-specific antimicrobial (biocidal) effect of the synthesized surfactant can be attributed to an electrostatic interaction between the the negatively charged cell membrane (lipoprotein) and the positively charged surfactant's ammonium group ( $R_4N^+$ ). Moreover physical disruption of the bacterial cell occurs when the surfactant's hydrophobic chain penetrates into the bacterial cell membrane. Penetration of the cell membrane leads to damage of the selective permeability of the cell, and then death of the bacterial cell (as previously described with the environmental sulfidogenic bacteria).

#### Relationship Between the Surface Activity and Corrosion Inhibition Efficiency

In general, the corrosion inhibition efficiency of synthesized surfactants depends on their ability to adsorb onto the metal surface. This adsorption leads to the formation of a protective layer over the metal surface. Therefore the CMC

plays a key role in determining the effectiveness of the synthesized surfactant as a corrosion inhibitor. When the corrosion inhibitor concentration reaches the  $C_{CMC}$ , an adsorbed layer of inhibitor covers the largest possible area on the mild steel surface according to stereochemistry of a synthesized surfactant. Adding more surfactant molecules to the solution combines to form micelles in the bulk solution [51]. On the basis of this view, the studied surfactant NCGS at low  $C_{CMC}$  showed high corrosion inhibition efficiency. On the other hand, it shows that the highest reduction in the surface tension (effectiveness,  $\pi_{CMC}$ ) was accompanied by high corrosion inhibition efficiency. In addition it is noted that the maximum surface access ( $\Gamma_{max}$ ) of NCGS is proportional to the corrosion inhibition efficiency.

## Conclusions

1. One novel cationic gemini surfactant was synthesized, characterized and successfully used to protect a metal surface from the medium salinity (inhibitor) and the sulfidogenic activities (biocide).
2. The novel cationic gemini surfactant (NCGS) showed good surface active properties at a low concentration.
3. The biocidal activity of the synthesized surfactant was achieved by preventing sulfide production and dropping of the redox potential in the bulk phase. This means all sulfidogenic bacterial communities in the bulk phase and over the metal surface were completely inhibited.
4. The NCGS showed high metal corrosion inhibition efficiency of 97 % at a concentration of 5 mM with environmental sulfidogenic bacteria growing at a medium salinity of 5.49 % NaCl.
5. The inhibition activity was achieved by protecting the metal surface from the biofilm development especially at a concentration of 0.1 mM NCGS.
6. Biocidal effect of the synthesized surfactant was related to the interaction of the surfactant molecules with the sulfidogenic bacterial cell membrane which leads to the death of the bacterial cell.
7. The high corrosion inhibition efficiency of the synthesized NCGS was related to the high adherent adsorption of the surfactant molecules on the metal surface and thus forming a protective film as confirmed by a scanning electron microscopy (SEM) image.
8. The synthesized NCGS showed a nonspecific antibacterial activity against Gram-positive and Gram-negative standard strains in comparison to tetracycline antibiotic.

## References

1. Bonnel A, Dabosi F, Deslouis C, Duprat M, Keddam M, Tribollet B (1983) Corrosion study of a carbon steel in neutral chloride solutions by impedance techniques. *J Electrochem Soc* 130:753–761
2. Sridhar N, Brossia CS, Dum DS, Anderko A (2004) Prediction localized corrosion in seawater. *Corrosion* 60:915–934
3. Videla HA (2000) An overview of mechanisms by which sulfate-reducing bacteria influence corrosion of steel in marine environments. *Biofouling* 15:37–47
4. Madsen BW, Cramer SD, Collins WK, Watson SW, Higdem D, Perkins W (1995) Corrosion in a phosphate slurry pipeline. *Mater Perform* 34:70–73
5. Stoodley P, Sauer K, Davies DG, Costerton JW (2002) Biofilms as complex differentiated communities. *Ann Rev Microbiol* 56:187–209
6. Geesey G, Beech I, Bremer P, Webster BJ, Wells WB (2000) Biocorrosion. In: Bryers JD (ed) *Biofilms II: process analysis and applications*. Wiley-Liss, New York, pp 281–325
7. Giudice C, Amo BD (1996) *Corrosion prevention and control*, pp 43–47
8. Badawi AH, Hegazy MA, El-Sawy AA, Ahmed HM, Kamel WM (2010) Novel quaternary ammonium hydroxide cationic surfactants as corrosion inhibitors for carbon steel and as biocides for sulfate-reducing bacteria (SRB). *Mater Chem Phys* 124:458–465
9. Rosen MJ (1989) *Surfactants and interfacial phenomena*, 2nd edn. Wiley, New York
10. Zhou M, Zhao J, Hu X (2012) Synthesis of Bis[*N*, *N*-(alkylamidoethyl)ethyl] triethylenediamine bromide surfactants and their oilfield application investigation. *J Surf Deterg* 3:309–315
11. Hegazy MA, Abdallah M, Ahmed H (2010) Novel cationic gemini surfactants as corrosion inhibitors for carbon steel pipelines. *Corrosion Sci* 52:2897–2904
12. Hegazy MA, Ahmed HM, El-Tabei AS (2011) Investigation of the inhibitive effect of *p*-substituted 4-(*N*, *N*, *N*-dimethyldodecylammonium bromide)benzylidene-benzene-2-yl-amine on corrosion of carbon steel pipelines in acidic medium. *Corros Sci* 53:671–678
13. Khaled KF, Hackerman N (2003) Investigation of the inhibitive effect of ortho-substituted anilines on corrosion of iron in 1 M HCl solutions. *Electrochim Acta* 48:2715–2723
14. Gamboa C, Olea AF (2006) Association of cationic surfactants to humic acid, effect on the surface activity. *Colloids Surf A* 278:241–245
15. Mata J, Varade D, Bahadur P (2005) Aggregation behavior of quaternary salt based cationic surfactants. *Thermochim Acta* 428:147–155
16. Samakande A, Chaghi R, Derrien G, Charnay C, Hartmann PC (2008) Aqueous behavior of cationic surfactants containing a cleavable group. *J Colloid Interface Sci* 320:315–320
17. Postgate JR (1984) *The sulfate reducing bacteria*, 2nd edn. Cambridge University Press, London, pp 30–100
18. Miller TL, Wolin MJ (1974) A serum bottle modification of the Hungate technique for cultivating obligate anaerobes. *Appl Microbiol* 27:985–987
19. DEV, Deutsche Einheitsverfahren zur Wasser (1993) *Abwasser und Schlammuntersuchung—Physikalische, chemische, biologische und bakteriologische Verfahren* (German Standard Methods for the Examination of Water, Wastewater and Sludge physical, chemical, biological and bacteriological methods), DIN Deutsches Institut für Normung e. V. Beuth
20. Singare PU, Mhatre JD (2012) Development of arginine based mono-peptides as cationic surfactants from pure amino acid. *Sci Technol* 2:55–60

21. Anonymous (1998) Multiple tube fermentation technique for members of the coli form group. In: Greenberg AE, Clesceri LS, Eaton AD (eds) Standard methods for the examination of water and wastewater. American Public Health Association, American Water Works Association, and Water Environment Federation, New York, pp 9–51
22. Quraishi MA, Ansari FA, Jamal D (2002) Thiourea derivatives as corrosion inhibitors for mild steel in formic acid. *Mater Chem Phys* 77:687–690
23. Khaled KF, Amin MA (2009) Electrochemical and molecular dynamics simulation studies on the corrosion inhibition of aluminum in molar hydrochloric acid using some imidazole derivatives. *J Appl Electrochem* 39:2553–2568
24. Neu TR (1996) Significance of bacterial surface-active compounds in interaction of bacteria with interfaces. *Microbiol Rev* 60:151–166
25. Lawrence JR, Swerhone GDW, Leppard GG, Araki T, Zhang X, West MM, Hitchcock AP (2003) Scanning transmission X-ray, laser scanning, and transmission electron microscopy mapping of the exopolymeric matrix of microbial biofilms. *Appl Environ Microbiol* 69:5543–5554
26. North AJ (2006) Seeing is believing? A beginners' guide to practical pitfalls in image acquisition. *J Cell Biol* 172:9–18
27. Wagner M, Ivleva NP, Haisch C, Niessner R, Horn H (2009) Combined use of confocal laser scanning microscopy (CLSM) and Raman microscopy (RM): investigations on EPS-Matrix. *Water Res* 43:63–76
28. Perez C, Pauli M, Bazerque P (1990) An antibiotic assay by agar-well diffusion method. *Acta Biol Med Exp* 15:113–115
29. Hegazy MA (2009) A novel Schiff base-based gemini surfactants: synthesis and effect on corrosion inhibition of carbon steel in hydrochloric acid solution. *Corros Sci* 51:2610–2618
30. Badawi AM, Mekawi MA, Mohamed AS, Mohamed MZ, Khowdairy MM (2007) Surface and biological activity of some novel cationic surfactants. *J Surf Deterg* 10:243–255
31. Gasol J, Casamayor E, Joint I, Garde K, Gustavson K, Benloch S, Díez B, Schauer M, Massana R, Pedrós-Alió C (2004) Control of heterotrophic prokaryotic abundance and growth rate in hypersaline planktonic environments. *Aquat Microb Ecol* 34:193–206
32. Voordouw G, Voordouw JK, Jack TR, Foght J, Fedorak PM, Westlake DWS (1992) Identification of distinct communities of sulfate-reducing bacteria in oil fields by reverse sample genome probing. *Appl Environ Microbiol* 58:3542–3552
33. Muyzer G, Stams AJM (2008) The ecology and biotechnology of sulfate-reducing bacteria. *Nat Rev Microbiol* 6:441–453
34. Lee WC, Lewandowski Z, Nielsen PH, Hamilton A (1995) Role of sulfate-reducing bacteria in corrosion of mild steel. A review. *Biofouling* 8:165–194
35. Brunt KD (1987) In: Hill HC (ed) Biocides for the oil industry, Wiley, New York, p 201
36. Ashassi-Sorkhabi H, Asghari E (2009) Influence of flow on the corrosion inhibition of St52-3 type steel by potassium hydrogen-phosphate. *Corros Sci* 51:1828–1835
37. Gonzalez Y, Lafont MC, Pebere N, Chatainier G, Roy J, Bouissou T (2005) A corrosion inhibition study of a carbon steel in neutral chloride solutions by zinc salt/phosphoric acid association. *Corros Sci* 37:1823–1837
38. Fang HP, Xu L-CH, Chan K-Y (2002) Effects of toxic metals and chemicals on biofilm and biocorrosion. *Water Res* 36:4709–4716
39. Werner SE, Johnson CA, Laycock NJ, Wilson PT, Webster BJ (1998) Pitting of type 304 stainless steel in the presence of a biofilm containing sulphate reducing bacteria. *Corros Sci* 40:465–480
40. González JEG, Santana FJH, Mirza-Rosca JC (1998) Effect of bacterial biofilm on 316 SS corrosion in natural seawater by EIS. *Corros Sci* 40:2141
41. Skolink AK, Hughes WC, Augustine BH (2000) A metallic surface corrosion study in aqueous NaCl solution using Atomic Force Microscopy (AFM). *Chem Education* 5:8–13
42. Thangavel K, Rengaswamy NS (1998) Relationship between chloride/hydroxide ratio and corrosion rate of steel in concrete. *Cem Concr Compos* 20:283–292
43. Von Wolzogen Kuhr CAH, Van der Vlugt IS (1934) Graphitization of cast iron as an electrochemical process in anaerobic soils. *Water* 18:147–165
44. Sanders PF, Hamilton WA (1983) Biological and corrosion activities of sulphate-reducing bacteria in industrial process plant. In: Dexter SC (ed) Biologically induced corrosion. NACE International, Houston, pp 47–68
45. Little B, Wagner P, Mansfeld F (1992) An overview of micro-biologically influenced corrosion. *Electrochim Acta* 37:2185–2194
46. Braissant O, Decho AW, Dupraz C, Glunk C, Przekop KM, Visscher PT (2007) Exopolymeric substances of sulfate-reducing bacteria: interaction with calcium at alkaline pH and implication for formation of carbonate minerals. *Geobiology* 5:401–411
47. Koch GH, Brongers MPH, Thompson NG, Virmani YP, Payer JH (2002) Corrosion costs and preventative strategies in the United States. Federal Highway Administration. Publication No. FHWA-RD-01-156. Printed in a supplemental to materials performance. NACE International
48. Sastri VS (1998) Corrosion inhibitor, vol 373. Wiley, New York, pp 39–40
49. Farhat AA, Quraishi MA (2010) Inhibitive performance of gemini surfactants as corrosion inhibitors for mild steel in formic acid. *Portugaliae Electrochimica Acta* 28:321–335
50. Rosen MJ, Li F, Morrall SW, Versteeg DJ (2001) The relationship between the interfacial properties of surfactants and their toxicity to aquatic organisms. *Environ Sci Technol* 35:954–959
51. Hegazy MA, El-Tabei AS, Bedair AH, Sadeq MA (2012) An investigation of three novel nonionic surfactants as corrosion inhibitors for carbon steel in 0.5 M H<sub>2</sub>SO<sub>4</sub>. *Corros Sci* 54:219–230

### Author Biographies

**Dr. rer. nat. Ahmed Labena** is a researcher at the Chair of Urban Water Systems Engineering, Technical University of Munich, Germany.

**Dr. Mohamed A. Hegazy** is an associate professor at the Egyptian Petroleum Research Institute (Petrochemicals Department, Surfactant Laboratory), Egypt.

**Prof. Dr. rer. nat. Harald Horn** is a director of the chair of Water Chemistry and Water Technology, Engler-Bunte-Institut, Karlsruhe Institute of Technology (KIT), Germany.

**Dr. rer. nat. Elisabeth Müller** is a director of the biological laboratory, working group “Microbiological Systems” Chair of Urban Water Systems Engineering, Technical University of Munich, Germany.